Characterization of Enzyme Motions by Solution NMR Relaxation Dispersion
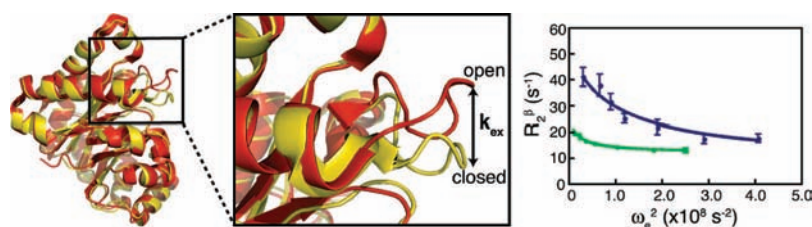
J. PATRICK LORIA,*,[†] REBECCA B. BERLOW,[‡] AND
ERIC D. WATT[†]

[†]Department of Chemistry, Yale University, New Haven, Connecticut 06520,
[‡]Department of Molecular Biophysics and Biochemistry, Yale University, New
Haven, Connecticut 06520

CONSPECTUS

In many enzymes, conformational changes that occur along the reaction coordinate can pose a bottleneck to the rate of conversion of substrates to products. Characterization of these rate-limiting protein motions is essential for obtaining a full understanding of enzyme-catalyzed reactions. Solution NMR experiments such as the Carr−Purcell−Meiboom−Gill (CPMG) spin-echo or off-resonance $R_{1\rho}$ pulse sequences enable quantitation of protein motions in the time range of microseconds to milliseconds. These experiments allow characterization of the conformational exchange rate constant, k_{ex}, the equilibrium populations of the relevant conformations, and the chemical shift differences ($\Delta\omega$) between the conformations.

The CPMG experiments were applied to the backbone N−H positions of ribonuclease A (RNase A). To probe the role of dynamic processes in the catalytic cycle of RNase A, stable mimics of the apo enzyme (E), enzyme−substrate (ES) complex, and enzyme−product (EP) complex were formed. The results indicate that the ligand has relatively little influence on the kinetics of motion, which occurs at 1700 s^{-1} and is the same as both k_{cat}, and the product dissociation rate constant. Instead, the effect of ligand is to stabilize one of the pre-existing conformations. Thus, these NMR experiments indicate that the conformational change in RNase A is ligand-stabilized and does not appear to be ligand-induced. Further evidence for the coupling of motion and enzyme function comes from the similar solvent deuterium kinetic isotope effect on k_{ex} derived from the NMR measurements and k_{cat} from enzyme kinetic studies. This isotope effect of 2 depends linearly on solvent deuterium content suggesting the involvement of a single proton in RNase A motion and function. Moreover, mutation of His48 to alanine eliminates motion in RNase A and decreases the catalytic turnover rate indicating the involvement of His48, which is far from the active site, in coupling motion and function.

For the enzyme triosephosphate isomerase (TIM), the opening and closing motion of a highly conserved active site loop (loop 6) has been implicated in many studies to play an important role in the catalytic cycle of the enzyme. Off-resonance $R_{1\rho}$ experiments were performed on TIM, and results were obtained for amino acid residues in the N-terminal (Val167), and C-terminal (Lys174, Thr177) portions of loop 6. The results indicate that all three loop residues move between the open and closed conformation at about 10 000 s^{-1}, which is the same as the catalytic rate constant. The O$^\gamma$ atom of Tyr208 provides a hydrogen bond to stabilize the closed form of loop 6 by interacting with the amide nitrogen of Ala176; these atoms are outside of hydrogen bonding distance in the open form of the enzyme. Mutation of Tyr208 to phenylalanine results in significant loss of catalytic activity but does not appear to alter the kex value of the N-terminal part of loop 6. Instead, removal of this hydrogen bond appears to result in an increase in the equilibrium population of the open conformer of loop 6, thereby resulting in a loss of activity through a shift in the conformational equilibrium of loop 6.

Solution NMR relaxation dispersion experiments are powerful experimental tools that can elucidate protein motions with atomic resolution and can provide insight into the role of these motions in biological function.

Introduction

The ability of enzymes to accelerate chemical reactions has intrigued scientists for nearly two centuries.[1] During an enzyme-catalyzed reaction, the structures of the substrates change as the enzyme converts them to intermediates, transition states, and finally products. It is not surprising that early in the study of enzymes it became clear that there were protein conformational changes occurring during the catalytic cycle. In many enzymes, the chemical reaction steps are not rate-limiting; instead, the slow step is a conformational change that presents a bottleneck to the conversion of substrate to product. Therefore, these rate-limiting time-dependent protein fluctuations must be characterized for a complete understanding of the physicochemical properties that govern the overall catalytic process. Solution NMR is unique in its ability to characterize protein motions over a wide range of biologically relevant time scales with atomic resolution. Here, we describe the use of two types of experiments, the relaxation-compensated Carr–Purcell–Meiboom–Gill (rcCPMG)[2] and the off-resonance rotating frame ($R_{1\rho}$) measurements,[3–5] that are suited for quantitative measurement of enzyme motions in the microsecond to millisecond time regimes. Fortunately, many enzyme catalytic rates (k_{cat}) range from 10^3 to 10^6 s^{-1} [6–8] and thus overlap nicely with the time scales accessible by these sensitive NMR experiments. There have been many excellent NMR dynamics studies on enzyme systems, but in keeping with the spirit of *Accounts of Chemical Research*, we focus on work performed in our laboratory. First, a brief review of the theory is presented, followed by some relevant aspects of experimental implementation of these relaxation schemes. Finally, the application to and insight gained from particular enzyme systems is presented.

Theory and Experimental Procedures

Space limitations preclude a detailed account of the NMR relaxation theory. However, this topic has been covered in-depth elsewhere,[9] and only the major points are described below. The following discussion focuses on an isolated two-spin (I–S) system (typically, ^{1}H–^{15}N or ^{1}H–^{13}C spin pairs) in which molecular motion is detected by monitoring the transverse relaxation rates of the ^{15}N or ^{13}C nuclei. Motion of a spin-1/2 nucleus between distinct magnetic environments on the aforementioned time scale is commonly referred to as conformational (or chemical) exchange. The conformational exchange process is subdivided into three categories—slow, intermediate, and fast—depending on whether the exchange rate constant (k_{ex}) is slower than, similar to, or faster than the chemical shift difference ($\Delta\omega$) between two exchanging conformations, which are commonly referred to as A and B. This

molecular motion disrupts the normal nuclear Larmor precession such that the observed resonance signal (Ω_{obs}) is broadened and in the intermediate and fast exchange cases resides at a population weighted average position,

$$\Omega_{obs} = p_A\Omega_A + p_B\Omega_B \tag{1}$$

in which $\Omega_{A/B}$ and $p_{A/B}$ are the chemical shifts and equilibrium populations for conformations A/B, and $\Delta\omega = \Omega_A - \Omega_B$. The extent of broadening of the NMR resonance depends on $k_{ex} = (k_1 + k_{-1})$, $p_{A/B}$, and $\Delta\omega$ for the exchange process, in which $k_{1/-1}$ are the forward and reverse rate constants. This additional *exchange* broadening of the resonance signal indicates an increase in the transverse relaxation rate, R_2, and suggests that measurement of R_2 can facilitate quantitation of the exchange parameters. Measurement of R_2 can be performed either by measuring the decay of the NMR resonance signal during a CPMG[10] (τ_{cp}–180°–τ_{cp}) type sequence where τ_{cp} is a delay that surrounds a 180° degree radio frequency (RF) pulse or by measuring the signal decay in the presence of an off-resonance, continuous wave spin-locking RF pulse ($R_{1\rho}$). In the former case, the measured relaxation rate $R_2(1/\tau_{cp})$ in the slow to intermediate exchange case depends in a complex manner on the exchange parameters and τ_{cp}.[11] In the limit of fast exchange, a simplified dependence of R_2 on the CPMG pulse spacing can be used.[12]

$$R_2(1/\tau_{cp}) = R_2^0 + \varphi_{ex}/k_{ex}[1 - 2\tanh(k_{ex}\tau_{cp}/2)/(k_{ex}\tau_{cp})] \tag{2}$$

It should be noted that in the fast limit, the populations and $\Delta\omega$ cannot be determined without additional independent measurements.

In the presence of a spin-locking RF field, $R_{1\rho}$ relaxation is measured as a trigonometric combination of longitudinal (R_1) and transverse (R_2) magnetization as defined by[4]

$$R_{1\rho} = R_1\cos^2\theta + R_2^0\sin^2\theta + \frac{\varphi_{ex}k_{ex}}{k_{ex}^2 + \omega_e^2}\sin^2\theta \tag{3}$$

$R_{1\rho}$ is measured at varying θ and ω_e values; subsequently, R_2 can be extracted from eq 3 by independent measure of R_1. The dependence of R_2 on the conformational exchange parameters and the effective spin-locking field (ω_e) can be determined in the fast limit such that

$$R_2 = \frac{\varphi_{ex}k_{ex}}{k_{ex}^2 + \omega_e^2} + R_2^0 \tag{4}$$

For $R_{1\rho}$ relaxation when exchange is outside the fast limit an alternate equation should be used.[13] In eqs 2–4, $\varphi_{ex} = p_A p_B\Delta\omega^2$, $\omega_e = (\omega_1^2 + \Omega^2)^{1/2}$, $\theta = \arctan(\omega_1/\Omega)$ is the tilt angle of the effective spin-locking field, and ω_1 is the ampli-
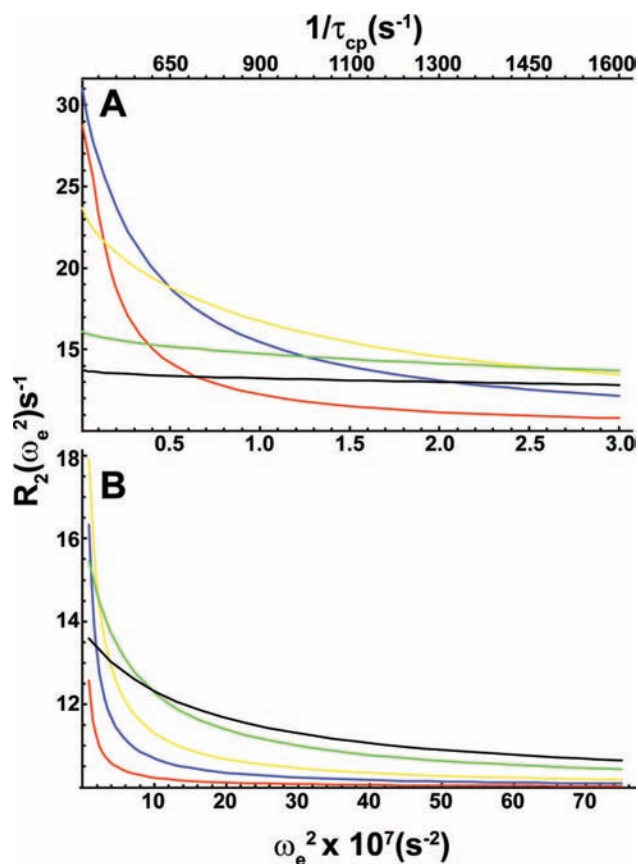
FIGURE 1. Range of accessible effective fields for dispersion experiments. Modeled relaxation dispersion curves for the rcCPMG (A) and $R_{1\rho}$ (B) experiments for an exchange process in which $p_A = 95\%$, $\Delta\omega = 1000$ s^{-1}, $R_2^0 = 10$ s^{-1}, and $k_{ex} = 500$ (red), 1500 (blue), 3000 (yellow), 7500 (green), and 12 500 s^{-1} (black). The lower *x*-axis indicates the effective field strength, whereas in panel A, the top *x*-axis depicts the more familiar τ_{cp} values used in CPMG experiments.

tude of the spin-locking field. In the CPMG experiment, the value of τ_{cp} is related to an effective field as well, described by $\omega_e = 12^{1/2}/\tau_{cp}$.[14]

In both the CPMG-type and $R_{1\rho}$ experiments, measurement of the variation in R_2 with ω_e is known as dispersion analysis. In both cases, the R_2 value varies because the applied effective field interferes with the spin dephasing caused by the conformational exchange process. Larger ω_e values are more effective at suppressing the effects of conformational exchange and thus the measured R_2 decreases with increasing ω_e. An example of a typical R_2 dispersion curve for experimentally available effective fields is shown in Figure 1.

If protein motion is suspected to be involved in protein function, both the rcCPMG and the $R_{1\rho}$ experiments can be performed under limiting conditions of ω_e to assess whether R_2 varies as a function of effective field strength. For the rcCPMG experiment, the limiting cases are slow and fast pulsing; for the $R_{1\rho}$ experiment, the limiting cases are low and high effective field strengths. Significant differences in R_2 val-

ues between these limits are indicative of microsecond to millisecond motions and suggest that additional experiments may be warranted. Using the rcCPMG experiment, quantitation of exchange rate constants, populations, and chemical shift differences is performed by measuring R_2 at many τ_{cp} values. Similarly, the conformational exchange parameters can be obtained from the $R_{1\rho}$ experiment by determining R_2 at multiple effective field strengths.

Fitting of the appropriate exchange equations to the relaxation dispersion data allows quantitation of the motional parameters. Experiment and simulation have indicated that a robust estimate of k_{ex} (and other dynamics parameters) is obtained from experimental data acquired at two or more static magnetic fields[14–16] or for more than one spin coherence.[17] The need for experimental data at multiple magnetic fields arises from an undesirable correlation in the fit parameters[16] resulting in multiple acceptable solutions, only one of which is obviously correct. The use of relaxation data at two magnetic fields or for multiple nuclei largely removes this correlation resulting in a robust and unique solution to the exchange equations.

Applications

NMR relaxation dispersion experiments have been successfully used to characterize internal protein motions,[2,4,18–20] protein folding,[21–25] protein–ligand interactions,[26,27] and enzyme function.[28–37] In the latter case of enzyme dynamics, several systems have been studied extensively; below, we focus on studies originating in our laboratory about the functional role of protein motions in ribonuclease A (RNase A) and triosephosphate isomerase (TIM).

Ribonuclease A

RNase A is a 14 kDa monomeric enzyme that catalyzes the transphosphorylation of single-stranded RNA without the use of cofactors or metal ions. The active site is in a cleft between two halves of the enzyme (Figure 2). The enzyme has specificity for pyrimidines on the 3′ side of the bond to be cleaved and purines on the 5′ side of this bond. Kinetic experiments have indicated that the rate-limiting step in the reaction is product release,[38] and biophysical studies have shown that a conformational change in the enzyme accompanies ligand binding at the active site.[39] To characterize motion in RNase A and investigate a potential link to catalytic function, NMR relaxation dispersion experiments were performed on apo-RNase A. These experiments identified a two-site conformational exchange process at multiple regions throughout the enzyme occurring at a rate of exchange k_{ex} (k_{-1}) of 1700
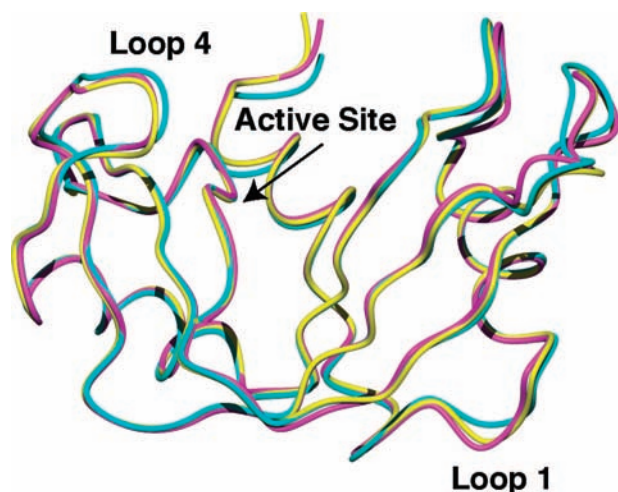
FIGURE 2. Ligand-dependent RNase A conformations. Ribbon representations of the apo[56] (yellow), E−pTppAp[29] (ES, cyan), and E−3′-CMP[57] (EP, magenta) structure of RNase A are shown in overlay view.
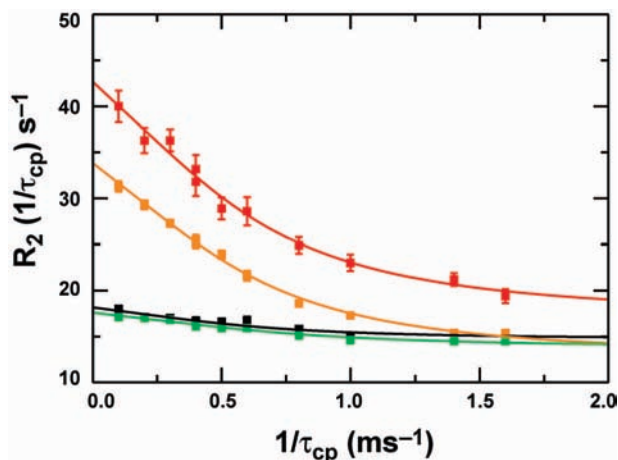

FIGURE 3. NMR evidence for motion in RNase A. rcCPMG dispersion curves collected at 14.1 T and 298 K for RNase A residues Ser16 (black), Thr17 (red), Asn71 (orange), and Thr100 (green).

(1615) s^{-1} (Figure 3).[28] Interestingly, this rate constant is identical to k_{cat} and to the product release (k_{off}) rate measured by NMR line shape analysis.[29] These studies suggested that motion in RNase A is coupled to the rate-limiting step (product release) in the catalytic process. Making a connection between protein motion and a particular aspect of the catalytic cycle is difficult, but below we outline one approach taken with RNase A to attempt to identify such a correlation.

The Effects of Ligand on Enzyme Structure. To address how the protein motions change as the enzyme performs its function, RNase A complexes with stable active site ligands that mimic the various substrate structures at stages along the enzyme's reaction coordinate were formed and subsequently studied by NMR. A noncleavable dinucleotide, phosphothymidine pyrophosphoryl adenosine phosphate (pTppAp), was used to mimic the enzyme's natural substrate, and 3′-CMP was chosen as a product-state mimic.[29,40] X-ray crystal structures of each enzyme form show distinct yet subtle structural changes (Figure 2). The alterations in backbone conformation going from the unliganded state to the ES complex are confined to active site loop 4, which provides purine specificity, and loop 1, located ~20 Å from the active site. Similar changes are observed in the EP complex, though for both loops the conformation is different than the E and ES forms. Having a structural basis for each complex allows more insight into the functional role of the motion observed by NMR. NMR relaxation measurements add another dimension to these structural studies by providing details regarding the motions in these time-averaged structures and by providing information on conformations lowly populated in small numbers that are in equilibrium with the dominant conformer, which is observed in solution and the crystal. These types of studies are described below.

The Effects of Ligand on the Conformational Exchange Process. As noted above, motion at multiple backbone positions in apo-RNase A occurs with a k_{ex} value of 1700 s^{-1}. Global fitting of the dispersion data at two static magnetic fields indicates that all of the flexible residues appear to move in a single, two-site exchange process.[29] The decision to fit all residues to a single, global exchange process rather than multiple independent processes is a difficult and complicated one.[29,37] In simple cases, the exchange data for all flexible residues are first fit independently. If the exchange rates are all similar, then a global process is assumed and all residues are treated as if they were involved in the same exchange process, resulting in single k_{ex} and p_A values and residue-specific $\Delta\omega$ values. We typically take a more tedious approach, in which statistical *F*-tests and Akaike information criteria (AIC) are used to compare the results of individual and global fits. Multiple rounds of this approach are performed by systematically removing individual data sets from the global model and subsequently comparing the results to the individual fits.[16,29] This type of analysis was performed with the RNase A example below.

In the RNase A ES complex, the exchange parameters are very similar to that seen in the apo form, both in spatial location and in measured k_{ex} values. Likewise, in the EP complex the rate constant and nature of the flexible residues is largely unchanged. The ligand-*independent* nature of the motional process, to a first approximation, tends to suggest a mechanistically similar motion in the E, ES, and EP complexes. This notion is supported by the similarity in Arrhenius profiles of k_{ex} versus temperature for E and ES complexes, which reveal similar activation barriers for this motion, ca. 5 kcal/mol.[29]
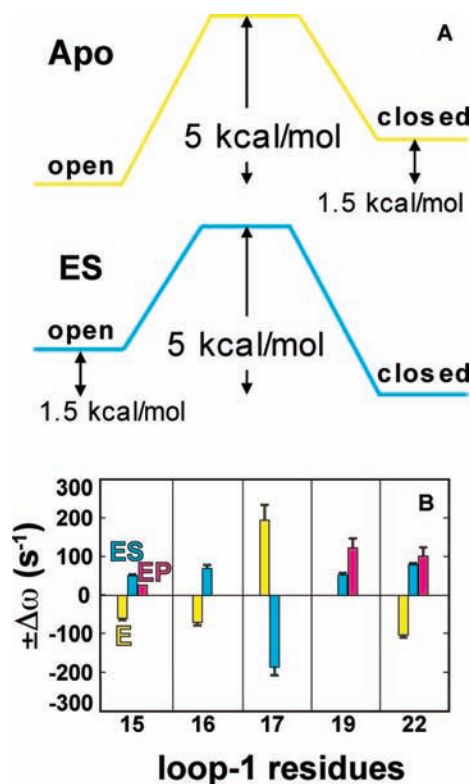
FIGURE 4. Thermodynamics and directionality of enzyme motion: (A) energy level diagram for apo and ES RNase A determined from Arrhenius profiles of k_{ex} versus temperature and measurement of p_A; (B) comparison of $\Delta\omega$ values for apo (yellow), ES (cyan), and EP (magenta) residues in loop 1.

Moreover, the populations of the major conformation are all similar for the E, ES, and EP complexes, ranging from 93% to 95%. Cumulatively, these data suggest that motion in RNase A is a two-site process and that ligand binding simply shifts the conformational equilibrium between the two species. We denote these two conformations as open (apo) and closed (ligand-bound) based on ultrasonic velocimetry measurements[41] that indicate compaction of the RNase A structure in the presence of ligand. Thus it appears that RNase A has evolved to sample a structure similar to the ES complex even in the absence of ligand (Figure 4) and it does so at an exchange rate constant that is equivalent to k_{cat}. These data imply that enzyme turnover and protein motion are coupled; however, an important question remains with regard to which structures are interconverting. Some insight into the structures of the equilibrium conformations can be obtained from the NMR experiments via $\Delta\omega$.[21]

Chemical Shift Comparison. A hypothesis, consistent with the data presented, is that RNase A exists in two conformations and that ligand binding either stabilizes the closed form or selects it from the equilibrium open and closed populations. If this hypothesis were true, then $\Delta\omega$ values from the

rcCPMG measurements on the apo form should be of equal magnitude and opposite sign of $\Delta\omega$ values determined from the E–pTppAp complex. The magnitude of $\Delta\omega$ is determined from the CPMG dispersion experiments, whereas the sign of $\Delta\omega$ can be obtained by comparison of HSQC and HMQC peak positions or by the static field dependence of HSQC resonances as described by Kay and co-workers.[42] The results of this analysis for loop 1 amino acid residues are depicted in Figure 4B.[29] For a handful of residues in loop 1, the $\Delta\omega$ values are consistent with the apo enzyme sampling the "substrate-bound conformation" in the absence of substrate. Likewise, the ES complex consists of a small population of open conformer even with substrate bound at the active site; the kinetics and structures of the exchange process are not perturbed by the ligand, only the populations.

For this comparison, the analysis of $\Delta\omega$ values was restricted to those in loop 1, that is, distant from the active site. The reason for this is that in the E–pTppAp (ES) complex, the chemical shifts for residues at the active site likely have significant electrostatic contributions from the negatively charged ligand and therefore are not a purely *conformational* $\Delta\omega$. In contrast, the $\Delta\omega$ values at the active site in the apo enzyme result only from changes in protein structure; therefore, any comparison of $\Delta\omega_{apo}$ with $\Delta\omega_{ES}$ for active site residues is extremely complicated. Nonetheless, comparison of $\Delta\omega$ values for residues in loop 1, being 20 Å from the bound ligand, are not likely to be affected by factors other than protein conformation and are consistent with the view that RNase A has evolved to sample the next relevant conformation on the catalytic cycle. This model is similar to conclusions from NMR studies of motion and function in dihydrofolate reductase,[34] triosephosphate isomerase (TIM),[43] and cyclophilin A.[35]

Biochemical Characterization. Thus far the idea that motion and function are coupled in RNase A has relied mainly on the NMR results presented above. If a true relationship exists, it is reasonable to expect that perturbation of the function may be reflected in concomitant changes in the NMR-measured motions. Two approaches were taken to investigate this, site-directed mutagenesis and alteration of solution conditions. In one example, aspartic acid 121 was mutated to alanine. In wild-type (WT) enzyme, this residue is completely conserved, presumably due to its interaction with the catalytic acid, His119. In the D121A mutant, the k_{off} for product is increased to 2500 s^{-1}.[30] NMR relaxation dispersion experiments with D121A show a commensurate increase in k_{ex} for the flexible backbone residues. In this mutant there is a decrease in k_{cat}, likely due to loss of productive interactions between Asp121 and His119 and a disruption of coordinated motions. Additional

mutation studies of His48, a conserved residue 18 Å from the active site, show a loss of protein motion in much of RNase A, a decrease in k_{cat} and alterations in k_{off} values.[44] These observations support the model in which there is a close connection between motions and the rate-limiting product release step. However, the absence of a 1:1 correlation between changes in k_{cat}, k_{off}, and k_{ex} demonstrate the complexity of protein motions in enzyme function.

Because motions in RNase A likely involve reorganization of hydrogen bonds, it is reasonable to expect that substituting D_2O for H_2O as the protein solvent would result in an isotope effect on k_{ex}. Experiments carried out at varying D_2O concentrations revealed a kinetic solvent isotope effect (KSIE) on k_{ex} of ~2, demonstrating the role of exchangeable proton(s) in enzyme motions.[31] Linear proton inventory experiments[45] indicate that a single dominant proton, associated with His48,[44] is involved in this motion. Interestingly, the isotope effect on protein motion is the same as the observed KSIE for k_{cat} and further strengthens the argument for a close coupling between motion and function in this enzyme. These experiments summarize a combined NMR and biochemical approach toward investigating the role of protein motion in enzyme function. The KSIE studies demonstrate that it is possible to localize the amino acid residue(s) involved in the rate-limiting protein motions out of a vast number of solvent-exchangeable sites.

Triosephosphate Isomerase (TIM)

Many enzymes are much larger than RNase A and pose significant challenges to study by solution NMR techniques. The approach taken to overcome some of these obstacles is presented in the following. TIM is a 53 kDa homodimeric enzyme that catalyzes the fifth step of glycolysis, the interconversion of dihydroxyacetone phosphate (DHAP) and glyceraldehyde-3-phosphate (GAP). Optimal function of triosephosphate isomerase relies on the ability of an active site Ω-loop (loop 6) to move between open and closed conformations (Figure 5A).[32,46] Motion in loop 6 is mediated by flexible hinge regions at the N- and C-termini of the loop. The closed conformation of the enzyme is stabilized by hydrogen bonds between loop 6 and neighboring loop 7. Loop 6 has been shown to move between open and closed conformations regardless of the enzyme's ligation state, with the populations skewed toward the open conformation in the absence of substrate and being mainly closed when substrate is bound.[43,47] Catalysis occurs in the closed loop conformation; in the physiologically important DHAP to GAP direction loop 6 opening
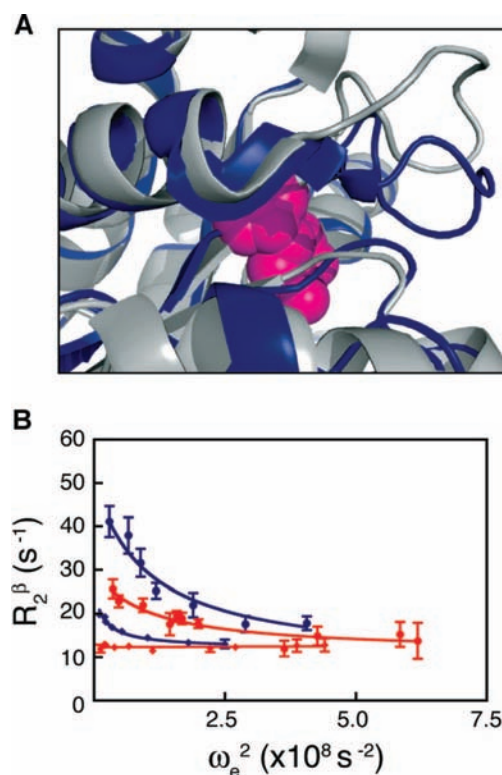

FIGURE 5. TIM loop motion: (A) open (gray) and closed (blue) conformations of the TIM active site; the catalytic residue Glu165 is highlighted in magenta; (B) $R_{1\rho}$ dispersion curves for Val167 (●) and Thr177 (◆) for WT (blue) and Y208F (red) TIM. All curves represent the best fit to a global, two-site exchange model, with the exception of Thr177 in Y208F, which is fit to a linear function with a slope of zero. Panel A was prepared using MacPyMOL.[58]

is partially rate-limiting, and therefore its motion has a direct impact on catalytic turnover.[48]

The large size of TIM presents resolution and signal-to-noise problems due to the long rotational correlation time (30 ns at 293 K) of the molecule. Deuteration[49] and transverse relaxation-optimized spectroscopy (TROSY)[50] techniques were necessary to provide the required sensitivity and resolution for thorough solution NMR studies. These approaches in addition to recently developed TROSY-based relaxation experiments[51−53] provided an avenue for the characterization of the motion of the active site loop in TIM as described below.

The Role of a Hydrogen Bond in Loop Motion. In wild-type TIM, a hydrogen bond between the amide nitrogen of Ala176 (in loop 6) and the O^η of Tyr208 (in loop 7) stabilizes the closed conformation of the enzyme. In the Y208F TIM mutant, this hydrogen bond is absent, and the catalytic efficiency of the enzyme (k_{cat}/K_m) is 2400-fold less than that of wild-type, indicating that the ability to stabilize the closed form of the enzyme is essential for optimal catalysis.[54] To accurately characterize loop motion in wild-type and mutant enzymes, relaxation dispersion experiments were carried out.

Because loop 6 motion is faster than motions observed in RNase A, $R_{1\rho}$ experiments of the TROSY variety[52] were necessary to quantitate the opening/closing process in WT and Y208F TIM. TROSY-selected $R_{1\rho}$[52] dispersion curves for the N- and C-terminal residues of loop 6 for WT and Y208F are shown in Figure 5B. The results show motion for both ends of loop 6 in WT on the 100 μs time scale ($k_{ex} = 8900$ s^{-1}). The site-specific nature of NMR spectroscopy allows the investigator to ask whether the observed flexible residues move in an independent fashion or as a group in a concerted process. In studies with TIM, similar to the RNase A example, this issue was addressed by comparing the fit statistics via *F*-test for individual and global motional models. The results for wild-type TIM indicate that the best description of motion for residues in both hinges of loop 6 is a global model in which all residues possess the same k_{ex} value (8900 s^{-1}).

The motion of the N-terminus of loop 6 in Y208F is similar to that observed for WT with $k_{ex} = 10\,000$ s^{-1}; however, the C-terminal residues in Y208F (Lys174 (not shown) and Thr177) have flat $R_{1\rho}$ dispersion curves and indicate that motion of these residues is outside the range of experimental measurement, likely due to highly skewed populations.[33] These NMR experiments show that removal of this hydrogen bond disrupts motion in one half of the loop more so than the other. This work demonstrates that detailed aspects of motion along the protein backbone can be obtained for larger enzyme systems. Recent experimental work focusing on methyl side chain positions demonstrates that information of the type described in this Account can be obtained for enzymes in the 300 kDa range.[55]

Conclusions

The atomic resolution and sensitivity to motion on a wide range of time scales makes solution NMR spectroscopy a unique tool for studying protein dynamics by providing information that is not as forthcoming from other experimental techniques. The ability of NMR relaxation dispersion experiments to quantitate kinetic processes (from measurement of k_{ex}) and thermodynamics (by estimation of conformer populations) enables keen insight into protein function. Importantly, the determination of chemical shifts of the minor, often unobservable, conformation from $\Delta\omega$ is extremely powerful, and this analysis has been extended to three-site exchange processes.[19,23] We anticipate future efforts will include a combination of computational and biochemical experiments together with NMR relaxation dispersion to allow modeling of these lowly populated species in small numbers, affording an unprecedented view of enzyme function.

BIOGRAPHICAL INFORMATION

Patrick Loria received his B.S. degree in Chemistry from The George Washington University in Washington, D.C. and a Ph.D. in Biochemistry working with Tom Nowak at the University of Notre Dame. He was a NIH postdoctoral fellow with Professor Arthur Palmer at Columbia University until 2000. He joined the Chemistry faculty at Yale University in 2001. His research efforts focus on solution NMR and biochemistry for characterization of enzymes and proteins involved in bacterial pathogenesis.

Rebecca Berlow received her B.A. in Chemistry from the Johns Hopkins University in 2005. She is currently pursuing her Ph.D. in Molecular Biophysics and Biochemistry at Yale University in the laboratory of Patrick Loria. At present, her research focuses on characterizing allosteric mechanisms in prokaryotic response regulator proteins involved in antibiotic resistance, in addition to continuing studies on the role of motional processes in enzyme function.

Eric Watt received his B.S. in Chemistry from the University of Michigan in 2005. He is currently pursuing his Ph.D. in Chemistry at Yale University in the Loria laboratory. His current research focuses on utilizing NMR relaxation experiments to characterize protein dynamics and folding.

REFERENCES

1   Payen, A.; Persoz, J. F. Memoire sur la diastase, les principaux produits de ses reactions et leur applications aux arts industriels. *Ann. Chim. Phys.* **1833**, *53*, 73–92.

2   Loria, J. P.; Rance, M.; Palmer, A. G. A relaxation-compensated Carr—Purcell—Meiboom—Gill sequence for characterizing chemical exchange by NMR spectroscopy. *J. Am. Chem. Soc.* **1999**, *121*, 2331–2332.

3   Zinn-Justin, S.; Berthault, P.; Guenneugues, M.; Desvau, H. Off-resonance rf fields in heteronuclear NMR: Application to the study of slow motions. *J. Biomol. NMR* **1997**, *10*, 363–372.

4   Akke, M.; Palmer, A. G. Monitoring macromolecular motions on microsecond-millisecond time scales by $R_{1\rho}-R_1$ constant-relaxation-time NMR spectroscopy. *J. Am. Chem. Soc.* **1996**, *118*, 911–912.

5   Mulder, F. A. A.; de Graaf, R. A.; Kaptein, R.; Boelens, R. An off-resonance rotating frame relaxation experiment for the investigation of macromolecular dynamics using adiabatic rotations. *J. Magn. Reson.* **1998**, *131*, 351–357.

6   Wolfenden, R.; Snider, M. J. The depth of chemical time and the power of enzymes as catalysts. *Acc. Chem. Res.* **2001**, *34*, 938–945.

7   Miller, B. G.; Wolfenden, R. Catalytic proficiency: The unusual case of OMP decarboxylase. *Annu. Rev. Biochem.* **2002**, *71*, 847–885.

8   Silverman, R. B. *The organic chemistry of enzyme-catalyzed reactions*, 1st ed.; Academic Press: New York, 2000.

9   Palmer, A. G.; Kroenke, C. D.; Loria, J. P. Nuclear magnetic resonance methods for quantifying microsecond-to-millisecond motions in biological macromolecules. *Methods Enzymol.* **2001**, *339* (Part B), 204–238.

10 Meiboom, S.; Gill, D. Modified spin-echo method for measuring nuclear spin relaxation times. *Rev. Sci. Instrum.* **1958**, *29*, 688–691.

11 Carver, J. P.; Richards, R. E. A general two-site solution for the chemical exchange produced dependence of T_2 upon the Carr—Purcell pulse separation. *J. Magn. Reson.* **1972**, *6*, 89–105.

12 Luz, Z.; Meiboom, S. Nuclear magnetic resonance study of the protolysis of trimethylammonium ion in aqueous solution-order of the reaction with respect to solvent. *J. Chem. Phys.* **1963**, *39*, 366–370.

13 Trott, O.; Palmer, A. G., 3rd. R1rho relaxation outside of the fast-exchange limit. *J. Magn. Reson.* **2002**, *154*, 157–160.

14 Ishima, R.; Torchia, D. A. Estimating the time scale of chemical exchange of proteins from measurements of transverse relaxation rates in solution. *J Biomol NMR* **1999**, *14*, 369–372.

15 Millet, O. M.; Loria, J. P.; Kroenke, C. D.; Pons, M.; Palmer, A. G. The static magnetic field dependence of chemical exchange linebroadening defines the NMR chemical shift time scale. *J. Am. Chem. Soc.* **2000**, *122*, 2867–2877.

16 Kovrigin, E. L.; Kempf, J. G.; Grey, M.; Loria, J. P. Faithful estimation of dynamics parameters from CPMG relaxation dispersion measurements. *J. Magn. Reson.* **2006**, *180*, 93–104.

17 Korzhnev, D. M.; Kloiber, K.; Kay, L. E. Multiple-quantum relaxation dispersion NMR spectroscopy probing millisecond time-scale dynamics in proteins: theory and application. *J. Am. Chem. Soc.* **2004**, *126*, 7320–7329.

18 Massi, F.; Grey, M. J.; Palmer, A. G., 3rd. Microsecond timescale backbone conformational dynamics in ubiquitin studied with NMR R1rho relaxation experiments. *Protein Sci.* **2005**, *14*, 735–742.

19 Grey, M. J.; Wang, C.; Palmer, A. G., 3rd. Disulfide bond isomerization in basic pancreatic trypsin inhibitor: multisite chemical exchange quantified by CPMG relaxation dispersion and chemical shift modeling. *J. Am. Chem. Soc.* **2003**, *125*, 14324–14335.

20 Mulder, F. A.; Hon, B.; Mittermaier, A.; Dahlquist, F. W.; Kay, L. E. Slow internal dynamics in proteins: application of NMR relaxation dispersion spectroscopy to methyl groups in a cavity mutant of T4 lysozyme. *J. Am. Chem. Soc.* **2002**, *124*, 1443–1451.

21 Hill, R. B.; Bracken, C.; DeGrado, W. F.; Palmer, A. G. Molecular motions and protein folding: Characterization of the backbone dynamics and folding equilibrium of alpha D-2 using C-13 NMR spin relaxation. *J. Am. Chem. Soc.* **2000**, *122*, 11610–11619.

22 Lundstrom, P.; Akke, M. Off-resonance rotating-frame amide proton spin relaxation experiments measuring microsecond chemical exchange in proteins. *J Biomol. NMR* **2005**, *32*, 163–173.

23 Korzhnev, D. M.; Salvatella, X.; Vendruscolo, M.; Di Nardo, A. A.; Davidson, A. R.; Dobson, C. M.; Kay, L. E. Low-populated folding intermediates of Fyn SH3 characterized by relaxation dispersion NMR. *Nature* **2004**, *430*, 586–590.

24 Grey, M. J.; Tang, Y.; Alexov, E.; McKnight, C. J.; Raleigh, D. P.; Palmer, A. G., 3rd. Characterizing a partially folded intermediate of the villin headpiece domain under non-denaturing conditions: contribution of His41 to the pH-dependent stability of the N-terminal subdomain. *J. Mol. Biol.* **2006**, *355*, 1078–1094.

25 Tang, Y.; Grey, M. J.; McKnight, J.; Palmer, A. G., 3rd; Raleigh, D. P. Multistate folding of the villin headpiece domain. *J. Mol. Biol.* **2006**, *355*, 1066–77.

26 Mittag, T.; Schaffhausen, B.; Gunther, U. L. Direct observation of protein-ligand interaction kinetics. *Biochemistry* **2003**, *42*, 11128–11136.

27 Tolkatchev, D.; Xu, P.; Ni, F. Probing the kinetic landscape of transient peptide-protein interactions by use of peptide (15)n NMR relaxation dispersion spectroscopy: binding of an antithrombin peptide to human prothrombin. *J. Am. Chem. Soc.* **2003**, *125*, 12432–12442.

28 Cole, R.; Loria, J. P. Evidence for flexibility in the function of ribonuclease A. *Biochemistry* **2002**, *41*, 6072–6081.

29 Beach, H.; Cole, R.; Gill, M.; Loria, J. P. Conservation of μs - ms enzyme motions in the apo- and substrate-mimicked state. *J. Am. Chem. Soc.* **2005**, *127*, 9167–9176.

30 Kovrigin, E. L.; Loria, J. P. Enzyme dynamics along the reaction coordinate: Critical role of a conserved residue. *Biochemistry* **2006**, *45*, 2636–2647.

31 Kovrigin, E. L.; Loria, J. P. Characterization of the transition state of functional enzyme dynamics. *J. Am. Chem. Soc.* **2006**, *128*, 7724–7725.

32 Kempf, J. G.; Ju-yeon, J.; Ragain, C.; Sampson, N. S.; Loria, J. P. Dynamic requirements for a functional protein hinge. *J. Mol. Biol.* **2007**, *368*, 131–149.

33 Berlow, R. B.; Igumenova, T. I.; Loria, J. P. Value of a Hydrogen Bond in Triosephosphate Isomerase Loop Motion. *Biochemistry* **2007**, *46*, 6001–6010.

34 Boehr, D. D.; McElheny, D.; Dyson, H. J.; Wright, P. E. The dynamic energy landscape of dihydrofolate reductase catalysis. *Science* **2006**, *313*, 1638–1642.

35 Eisenmesser, E. Z.; Millet, O.; Labeikovsky, W.; Korzhnev, D. M.; Wolf-Watz, M.; Bosco, D. A.; Skalicky, J. J.; Kay, L. E.; Kern, D. Intrinsic dynamics of an enzyme underlies catalysis. *Nature* **2005**, *438*, 117–121.

36 Zhan, Y.; Rule, G. S. Glutathione induces helical formation in the carboxy terminus of human glutathione transferase A1-1. *Biochemistry* **2004**, *43*, 7244–7254.

37 McElheny, D.; Schnell, J. R.; Lansing, J. C.; Dyson, H. J.; Wright, P. E. Defining the role of active-site loop fluctuations in dihydrofolate reductase catalysis. *Proc. Natl. Acad. Sci. U.S.A.* **2005**, *102*, 5032–5037.

38 Hammes, G. G. Multiple conformational changes in enzyme catalysis. *Biochemistry* **2002**, *41*, 8221–8228.

39 Cathou, R. E.; Hammes, G. G. Relaxation spectra of ribonuclease. I. The interaction of ribonuclease with cytidine 3′-phosphate. *J. Am. Chem. Soc.* **1965**, *86*, 3240–3245.

40 Kovrigin, E. L.; Cole, R.; Loria, J. P. Temperature dependence of the backbone dynamics of Ribonuclease A in the ground state and bound to the inhibitor 5′-phosphothymidine (3′—5′) pyrophosphate adenosine 3′-phosphate. *Biochemistry* **2003**, *42*, 5279–5291.

41 Dubins, D. N.; Filfil, R.; Macgregor, R. B.; Chalikian, T. V. Role of water in protien-ligand interactions: Volumetric characterization of the binding of 2′-CMP and 3′-CMP to ribonuclease A. *J. Phys. Chem. B.* **2000**, *104*, 390–401.

42 Skrynnikov, N. R.; Dahlquist, F. W.; Kay, L. E. Reconstructing NMR spectra of "invisible" excited protein states using HSQC and HMQC experiments. *J. Am. Chem. Soc.* **2002**, *124*, 12352–12360.

43 Williams, J. C.; McDermott, A. E. Dynamics of the flexible loop of triosephosphate isomerase: the loop motion is not ligand gated. *Biochemistry* **1995**, *34*, 8309–8319.

44 Watt, E. D.; Shimada, H.; Kovrigin, E. L.; Loria, J. P. The mechanism of rate-limiting motions in enzyme function. *Proc. Natl. Acad. Sci. U.S.A.* **2007**, *104*, 11981–11986.

45 Gross, P.; Steiner, H.; Krauss, F. On the deomposition of diazo-acetic ester catalysed by protons and deutons. *Trans. Faraday Soc.* **1936**, *32*, 877–879.

46 Pompliano, D. L.; Peyman, A.; Knowles, J. R. Stabilization of a reaction intermediate as a catalytic device: Definition of the functional role of the flexible loop in triosephosphate isomerase. *Biochemistry* **1990**, *29*, 3186–3194.

47 Massi, F.; Wang, C.; Palmer, A. G., 3rd. Solution NMR and computer simulation studies of active site loop motion in triosephosphate isomerase. *Biochemistry* **2006**, *45*, 10787–10794.

48 Maister, S. G.; Pett, C. P.; Albery, W. J.; Knowles, J. R. Energetics of triosephosphate isomerase: the appearance of solvent tritium in substrate dihydroxyacetone phosphate and in product. *Biochemistry* **1976**, *15*, 5607–5612.

49 LeMaster, D. M. Chiral β and random fractional deuteration for the determination of protein sidechain conformation by NMR. *FEBS* **1987**, *223*, 191–196.

50 Pervushin, K.; Riek, R.; Wider, G.; Wuthrich, K. Attenuated T2 relaxation by mutual cancellation of dipole-dipole coupling and chemical shift anisotropy indicates an avenue to NMR structures of very large biological macromolecules in solution. *Proc. Natl. Acad. Sci. U.S.A.* **1997**, *94*, 12366–12371.

51 Wang, C.; Rance, M.; Palmer, A. G. Mapping chemical exchange in proteins with MW > 50 kD. *J. Am. Chem. Soc.* **2003**, *125*, 8968–8969.

52 Igumenova, T. I.; Palmer, A. G., 3rd. Off-resonance TROSY-selected R 1rho experiment with improved sensitivity for medium- and high-molecular-weight proteins. *J. Am. Chem. Soc.* **2006**, *128*, 8110–8111.

53 Kempf, J. G.; Jung, J.; Sampson, N. S.; Loria, J. P. Off-resonance TROSY (R1ρ - R1) for quantitation of fast exchange processes in large proteins. *J. Am. Chem. Soc.* **2003**, *125*, 12064–12065.

54 Sampson, N. S.; Knowles, J. R. Segmental motion in catalysis: investigation of a hydrogen bond critical for loop closure in the reaction of triosephosphate isomerase. *Biochemistry* **1992**, *31*, 8488–8494.

55 Sprangers, R.; Gribun, A.; Hwang, P. M.; Houry, W. A.; Kay, L. E. Quantitative NMR spectroscopy of supramolecular complexes: Dynamic side pores in ClpP are important for product release. *Proc. Natl. Acad. Sci. U.S.A.* **2005**, *102*, 16678–16683.

56 Wlodawer, A.; Svensson, L. A.; Sjolin, L.; Gilliland, G. L. Structure of phosphate-free ribonuclease A refined at 1.26 Å. *Biochemistry* **1988**, *27*, 2705–2717.

57 Zegers, I.; Maes, D.; Dao-Thi, M. H.; Poortmans, F.; Palmer, R.; Wyns, L. The structures of RNase A complexed with 3′-CMP and d(CpA): active site conformation and conserved water molecules. *Protein Sci.* **1994**, *3*, 2322–2339.

58 DeLano, W. L. DeLano Scientific LLC, South San Francisco, CA, 2005.